Article

Effect of Trace Water on the 1,2-Dichloroethane Cracking over Zeolite Catalysts

Quan Zhang, Wei Huang, Jiacheng Xing, Xingzong Dong, Guangye Liu, Yunpeng Xu,* and Zhongmin Liu

Read Online

ACCESS | Metrics & More | Article Recommendations | Supporting Information

ABSTRACT: 1,2-Dichloroethanes (EDCs) with different water contents were used as feedstock for the catalytic dehydrochlorination of 1,2-dichloroethane to produce a vinyl chloride monomer (VCM) reaction using zeolite catalysts. It was found that the presence of trace water had a significant negative impact on both the activity and stability of zeolite catalysts for the 1,2-dichloroethane catalytic cracking reaction. Various characterization tools and theoretical calculations confirm that the presence of trace water affects the active center of the zeolite and enhances the adsorption of VCM and EDC, resulting in the deactivation of the zeolite catalyst. This study provides useful ideas for the development of practical catalysts and the stable operation of industrial EDC catalytic cracking processes.
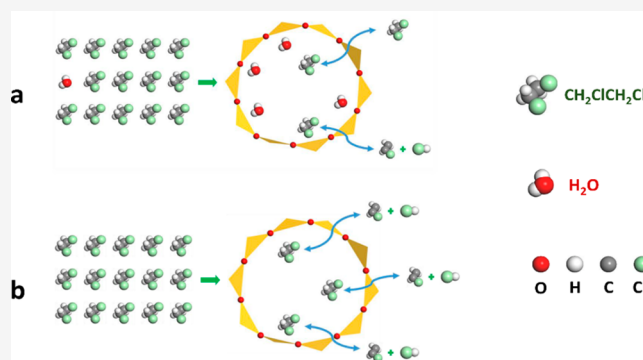
INTRODUCTION

Polyvinyl chloride (PVC) is one of the five major general plastics and plays a significant role in daily life and industrial processes. Vinyl chloride monomer (VCM) is currently the monomer used for the production of PVC, which is mainly produced by the direct hydrochlorination of acetylene[1] and ethylene chlorination to 1,2-dichloroethane (EDC), followed by EDC thermal cracking.[2] The EDC thermal cracking reaction has a high temperature and low efficiency, which needs to be replaced by a milder and more efficient technology.[3] Catalytic cracking of EDC to VCM has a high efficiency under relatively mild reaction conditions and is considered the most promising alternative technology to EDC thermal cracking.[2,4,5] Improving the activity and stability of catalysts is the focus of research in this field, but it is also a great challenge.[6]

Current EDC cracking catalysts mainly include metal chlorides,[7,8] metal oxides,[9,10] zeolites,[11,12] activated carbons,[6,13−15] and ionic liquids.[16] Among the numerous EDC cracking catalysts, zeolites have attracted the attention of researchers due to their high activity and regeneration capability.[12] Cook et al.[17] reported the application of zeolite catalysts in EDC cracking and proposed a correlation between the size of zeolite particles and the catalytic activity for EDC cracking. Shalygin[9] provided a detailed exploration of the catalytic mechanism of the HZSM-5 catalytic cracking of EDC to VCM with the Fourier transform infrared spectroscopy (FTIR). The study revealed that the catalytic efficiency of the Lewis acid of the zeolite was much higher than that of the

Bronsted acid center in this reaction. Oligomers in Bronsted acids were proven to be the main reason for catalyst deactivation.

There is no water involved in the EDC catalytic cracking reaction. However, current typical EDC industrial production is mainly achieved through the ethylene oxychlorination reaction, and water is simultaneously produced with the formation of the EDC product.[2] The water content requirement of chemically pure 1,2-dichloroethane in the National Standard of China (GB/T15895−2021) is ≤0.1%. Therefore, trace water is inevitably present in EDC products despite the subsequent rigorous dehydration process. The effect of trace water on the subsequent EDC reactions is easy to ignore in specific research work. To date, the effect of trace water in feedstocks on the catalytic cracking of EDC to produce VCM has not been reported. In this paper, the effect of trace water in EDC feedstocks on the reaction performance of zeolite catalysts was investigated, and the variation in zeolite acidity in the presence of water was explored by using various characterization tools, such as solid-state NMR, thermogravimetry, Py-FTIR, FTIR, and in situ feedstock switching tests. A theoretical calculation study was used to reveal the effect of

trace water on the catalytic cracking performance of zeolite catalysts.

EXPERIMENTAL SECTION

Materials. HZSM-5 (molar ratio, $SiO_2/Al_2O_3 = 35$, Nankai Catalyst Plant)

USY (molar ratio, $SiO_2/Al_2O_3 = 8$, Nankai Catalyst Plant)

1,2-Dichloroethane (Daimao Reagent Plant, water content: 181 ppm, 1203 ppm)

1,2-Dichloroethane (water content:73 ppm): 15 g of zeolites (3A) were placed in 500 mL of 1,2-dichloroethane (water content:181 ppm) for 12 h. The zeolites were removed, the above process was repeated twice, and the final reagent obtained is 1,2-dichloroethane with 73 ppm water.

1,2-Dichloroethane (water content: 20 ppm): 15 g of zeolites (3A) were placed in 500 mL of 1,2-dichloroethane (water content:181 ppm) for 12 h. The zeolites were removed, the above process was repeated four times, and the final reagent obtained is 1,2-dichloroethane with 20 ppm of water.

Characterization.

1. The powder XRD pattern was recorded on a PAN-alytical X'Pert PRO X-ray diffractometer with Cu-Ka radiation (l 1/4 0.15418 nm), operating at 40 kV and 40 mA.

2. The chemical composition of the solid samples was determined with a Philips Magix-601 X-ray fluorescence (XRF) spectrometer.

3. The crystal morphology was observed by scanning electron microscopy (Hitachi SU8020).

4. N_2 adsorption−desorption isotherms at −196 °C were determined on a Micromeritics ASAP 2020 system. Prior to the measurement, samples were degassed at 350 °C under a vacuum for 5 h. The total surface area was calculated based on the BET equation. The micropore volume and micropore surface area were evaluated using the t-plot method.

5. Temperature-programmed desorption of ammonia (NH_3-TPD) was measured on a Micromeritics 2920 chemical adsorption instrument of . Each sample (20−40 mesh, 0.15 g) was loaded into a stainless U-shaped micro reactor (i.d.= 5 mm) and pretreated at 600 °C for 1 h in flowing He. After the pretreatment, the sample was cooled to 100 °C and saturated with NH_3 gas. NH_3-TPD was then carried out in a constant flow of He (20 mL min^{-1}) from 100 to 700 °C at a heating rate of 20 °C/min.

6. Catalyst acidities were characterized by Fourier transform infrared spectroscopy with the adsorption of pyridine (Py-FTIR) on a Bruker Tensor 27 spectrometer with an MCT detector. It is divided into the following categories. (I) HZSM-5 (15 mg) was pressed into a self-supporting wafer and placed in a quartz cell. The samples were pretreated at 500 °C for 240 min under a vacuum and cooled to 300 °C. The spectrum of HZSM-5 without pyridine perturbations was collected. Afterward, the IR cell was saturated by water, the sample adsorbs water vapor for 5 min and evacuated for 30 min to remove physically adsorbed water. Afterward, the IR cell was saturated with pyridine and subsequently evacuated for 30 min to remove physically adsorbed pyridine. The spectrum of Py-FTIR was collected from 4000 to 1000 cm^{-1} by averaging 64 scans with a

resolution of 4 cm^{-1}. (II) HZSM-5 (15 mg) was pressed into a self-supporting wafer and placed in a quartz cell. The samples were pretreated at 500 °C for 240 min under a vacuum and cooled to 300 °C. The spectrum of HZSM-5 without pyridine perturbations was collected. Afterward, the IR cell was saturated with pyridine and subsequently evacuated for 30 min to remove physically adsorbed pyridine. The spectrum of Py-FTIR was collected from 4000 to 1000 cm^{-1} by averaging 64 scans with a resolution of 4 cm^{-1}.

7. Catalysts were characterized by Fourier transform infrared spectroscopy with adsorption of water on a Bruker Tensor 27 spectrometer with an MCT detector. HZSM-5 (15 mg) was pressed into a self-supporting wafer and placed in a quartz cell. The samples were pretreated at 500 °C for 240 min under a vacuum and cooled to 300 °C. The spectrum of HZSM-5 was collected. Afterward, the IR cell was saturated by water, the sample adsorbs water vapor for 5 min and evacuated for 30 min to remove physically adsorbed water. The spectrum of FTIR was then collected from 4000 to 1000 cm^{-1} by averaging 64 scans with a resolution of 4 cm^{-1}.

8. ^{13}C MAS NMR spectra were performed on a Bruker Avance III 600 spectrometer equipped with a 14.1 T wide-bore magnet using a 4 mm or 7 mm MAS probe. The resonance frequency was 150.9 MHz for 13C.

9. The water content was tested using a Karl Fischer analyzer.

10. The TG test was performed by the SDT Q600 thermal analyzer from TA, USA, for sample weight change and heat flow analysis. Analysis conditions: sample filling volume 15 mg, air atmosphere, air flow rate of 100 mL/min, temperature increase rate 10 °C/min.

Catalytic Evaluation. The catalytic dehydrochlorination of 1,2-dichloroethane to produce the vinyl chloride monomer reaction was carried out in a fixed bed reactor. The reactor selected was a quartz tube reactor with an inner diameter of $\varphi6$. Under atmospheric pressure conditions, the feed was fed by means of saturated vapor carried by nitrogen, the ambient temperature of 1,2-dichloroethane was 10 °C, the N_2 flow rate was 60 mL/min, and the catalyst mass was 1.59 g.

RESULTS AND DISCUSSION

Two typical zeolites, HZSM-5 and USY, were selected and investigated in this research. Figures S2−S4 show the XRD, SEM, and NH_3-TPD results of the selected zeolites. Zeolite HZSM-5 has characteristic Bragg reflections at 7.86, 8.77, 22.99, 23.21, 23.61, 23.84, and 24.30°. Zeolite USY has characteristic Bragg reflections at 6.28, 10.26, 12.04, 15.85, 20.61, 23.94, and 27.38°. These Bragg reflections peaks are consistent with the respective standard cards (JCPDS: 00−049−0657) (JCPDS: 01−077−1549). From Figures S3 and S4, it can be seen that the selected zeolites have good crystallinity with crystal sizes ranging from 0.5 to 2 μm, and both showed two types of classic acidic sites. The SiO_2/Al_2O_3 ratios, BET surface areas, and total pore volumes of the selected zeolites were also summarized in Table S1. The SiO_2/Al_2O_3 ratios of HZSM-5 and USY were 34.6 and 7.2, respectively. Both zeolites have large specific surface areas and microporous pore capacity characteristics. The EDC catalytic cracking performance of zeolite catalysts was
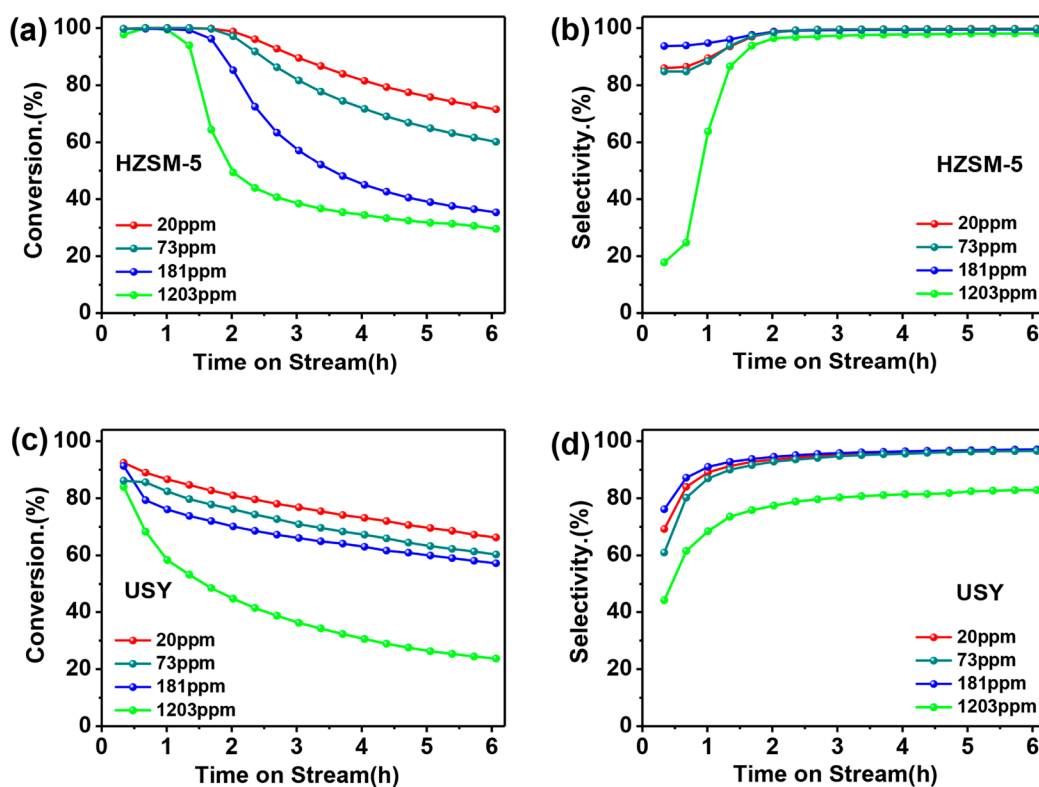
Figure 1. (a, c) EDC conversion and (b, d) the selectivity of VCM over zeolite catalysts under different water content EDCs as feedstocks. (a, b) WHSV = 0.5 h^{-1}, zeolite: HZSM-5; (c, d) USY, 300 °C, 0.1 MPa, N$_2$/CH$_2$ClCH$_2$Cl = 19/1. (Red curve, EDC (20 ppm water content); dark green curve, EDC (73 ppm water content); blue curve, EDC (181 ppm water content); light green curve, EDC (1203 ppm water content).).

investigated by using four EDC feedstocks with different water contents (1203, 181, 73, and 20 ppm).

As shown in Figure 1, the effect of different water contents in EDC feedstocks on the performance of the catalytic cracking of EDC using HZSM-5 or USY as catalysts was investigated. The results of the HZSM-5 catalyst (Figure 1a, b) showed that the conversion of EDC was maintained at 100% until 1.5 h of the reaction regardless of the water content in the EDC feedstocks. Subsequently, it gradually accelerated with increasing water content. In terms of VCM selectivity, the HZSM-5 catalyst had the lowest initial selectivity when EDC with a water content of 1203 ppm was used as the feedstock. As the reaction proceeded, the selectivity tended to be close to 100% for all feedstocks. In contrast, the results of the USY catalyst were different from those of the HZSM-5 catalyst, as shown in Figure 1c, d. It can be seen that the initial activity of USY is the highest activity for all the four different water contents of EDC as feedstock, compared to HZSM-5 maintained for a period of time. As the reaction proceeds, the activity of zeolite USY gradually decreases. The conversion of EDC is about 10% different when the water content of EDC is increased from 20 to 181 ppm. This indicates that USY has water resistance in comparison with HZSM-5. Once the water content increased to 1203 ppm, the difference in the activity of USY became more obvious. The catalytic activity of USY was substantially decreased. The VCM selectivity of the USY catalyst remained less than 80% during the reaction of 6 h when EDC with the water content of 1203 ppm was used as the feedstock, while others' selectivity was close to 100% after 2 h of reaction.

The stability of the two types of zeolite catalysts was further investigated and the results are shown in Figure S5. The EDC

conversion curves were plotted as slope curves to compare the stability difference between catalysts. The total conversion of EDC on HZSM-5 and USY decreased from 100% to about 60% and 92% to about 57%, respectively, when EDC with 20 ppm water content was feedstock. Meanwhile, when EDC with 1203 ppm water content was feedstock, the total conversion of EDC on HZSM-5 and USY decreased from 100% to about 25% and 83% to about 17% on EDC at 1203 ppm, respectively. In terms of the general trend, the stability of the zeolite catalyst in the EDC feedstock with 20 ppm water content was superior to that in the EDC feedstock with 1203 ppm water content. From the three slope curves, the presence of water particularly affects the first slope curve, and the next two slope curves are parallel to each other, showing that the deactivation rates of the two catalysts are similar in the later stages.

The noteworthy differences in the catalytic activity, selectivity, and stability on zeolite catalysts when using EDC feedstocks with different water contents indicate that the presence of trace water has a significant negative impact on the catalytic cracking of EDC to produce VCM. This result is different from previous reports indicating that the presence of water tends to facilitate catalytic cracking reactions.[18−20] This facilitation is mainly reflected in the fact that water molecules can reduce carbon deposition on the active site of zeolite catalysts and are also conducive to mass and heat transfer in the reaction process.[21−23] In addition to the promotion effect on the reaction performance, the presence of water also changes the acidic property of the zeolite catalyst, which has a positive or negative effect on the reaction performance, mainly depending on the mechanism of the catalyzed reaction.[24−26] Previous studies have shown that acidic species have an important effect on the catalytic cracking of EDC.[9] Based on

this, it was speculated that the presence of water in the feedstock might change the acidity or quantity of the zeolite catalyst and then change the catalytic performance in EDC cracking. A series of experiments and characterizations were carried out to reveal the effect of water on the catalytic performance of zeolites in the EDC cracking reaction.

The carbon depositions of selected zeolites after reaction for 10 h using two kinds of EDC (20 ppm, 1203 ppm) feedstocks were determined by thermogravimetry (Table 1, Figure S6).

Table 1. Mass Loss Amount from TG Results (Figure S5)

conditions	HZSM-5 (%)	USY (%)
20 ppm-10h	7.6	9.7
1203 ppm-10h	7.1	10.3

The TG curves showed little difference of about 0.5% in the amount of carbon deposition by the same catalyst under two kinds of EDC feedstocks. However, Figure 1 shows that the EDC conversions of the two feedstocks with water contents of 20 and 1203 ppm were extremely different. This means that the carbon deposition of selected zeolites using EDC feedstock with a water content of 1203 ppm was significantly more serious than that of EDC with a water content of 20 ppm compared with the unit EDC conversion. Notably, the composition of the carbon species in the zeolites used was probed using solid-state NMR techniques, and the chemical shifts of the carbon species in the zeolites with the same topological structure with EDC feedstock with different water contents remained essentially the same, as shown in Figure S7. According to Shalygin,[9] the formation of oligomers in Bronsted acids was the main reason for zeolite catalyst deactivation, indicating that the participation of water might lead to a change in zeolite acid sites during the reaction.

Based on the above, FTIR and Py-FTIR were used to further investigate whether water molecules affected the acid distribution of zeolite catalysts. The FTIR spectra of HZSM-5 (H) and USY (U) under aqueous and anhydrous conditions are shown in Figure S8, respectively. Compared with the anhydrous condition, the stretching vibration of Bronsted acid sites bridging hydroxyl groups at 3740 cm^{-1} was significantly reduced in the aqueous condition, while the stretching vibration peaks of the hydroxyl nests represented at 3700–3400 cm^{-1} are also obviously enhanced. These results indicated a reduction in the number of bridged hydroxyls and an increase in the number of hydroxyl nests in the zeolite frameworks in the presence of water.[27,28] It is generally believed that at high temperatures and in the presence of water, skeletal aluminum delamination occurs on zeolites, which leads to the formation of hydroxyl nests.[29,30] The hydrogen-bonded hydroxyl clusters formed by these framework defects are called hydroxyl nests. The defects caused by the first T atom are mainly to adjust the acidity of the zeolites, optimizing the catalytic and diffusion properties of the zeolites. Based on this, it is necessary to modify the structure of zeolites, such as high-temperature steam passivation and acid treatment. When defects have negative effects on the catalytic reaction of zeolites, silicon species need used to supplement the defects of zeolites to further eliminate the defect acidity.[30]

New findings were observed by Py-FTIR, as presented in Figure 2 and Table 2. First, we learned from the literature that the absorption peak of Py-FTIR at approximately 1540 cm^{-1} represents Bronsted acid sites and the absorption peak at 1460
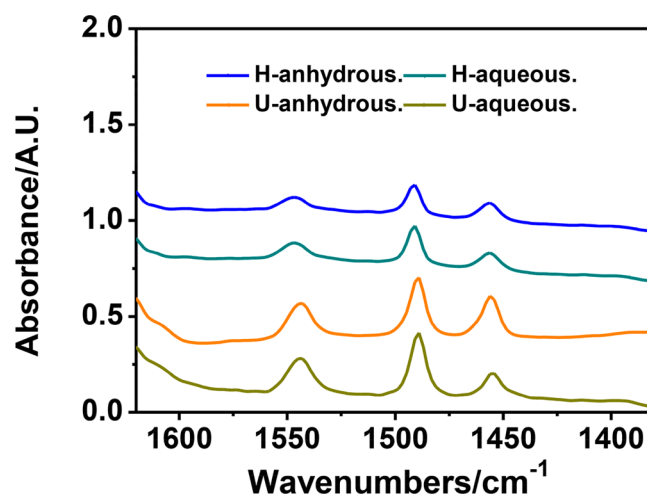

Figure 2. Py-FTIR of zeolites before and after water adsorption. (Blue curve, HZSM-5 under anhydrous conditions; navy blue curve, HZSM-5 under aqueous conditions; orange curve, USY under anhydrous conditions; yellow, USY under aqueous conditions.)

Table 2. Ratio of Bronsted Acid Sites to Lewis Acid Sites under Several Conditions[a]

conditions	HZSM-5	USY
anhydrous	1.47	1.69
aqueous	1.96	2.60
2 min-20 ppm	2.61	1.41
2 min-1203 ppm	1.62	0.61
20 min-20 ppm	2.69	1.44
20 min-1203 ppm	3.22	1.00

[a]The ratio is measured by Fourier transform infrared spectroscopy with the adsorption of pyridine.

cm^{-1} represents Lewis acid sites.[31] With the presence of water, the ratio of Bronsted acid sites to Lewis acid sites is significantly improved. This means that part of the nonframework aluminum is transformed into framework aluminum in the presence of water, Lewis acid sites can transform to Bronsted acid sites, one reversible change. Combining the results of the two IR spectra, the following conclusions can be drawn, showing that the existence of water can easily change the types of acid sites in zeolites. At 300 °C, the entry of water molecules achieves the dealumination of the molecular sieve skeleton and forms hydroxyl nests on the one hand, and the presence of water converts the Lewis acid to Bronsted acid on the other.

To quantitatively describe the change in the acid sites of zeolites caused by different water contents, we used Py-FTIR to analyze the catalysts after reaction for 2 and 20 min (Table 2). Compared to the results of EDC with a water content of 20 ppm, the ratio of the Bronsted acid sites to Lewis acid sites of the catalysts decreased after 2 min of reaction when EDC with a water content of 1203 ppm was used as the feedstock. However, when the EDC with a water content of 20 ppm was used as the feedstock, the ratio increased after 20 min of reaction compared with the result of 2 min of reaction. In contrast, the ratio for all zeolite catalysts remained essentially unchanged when EDC with a water content of 20 ppm was used as the feedstock. This result is in agreement with the results of previous characterizations (Figure S8, Figure 2, Table
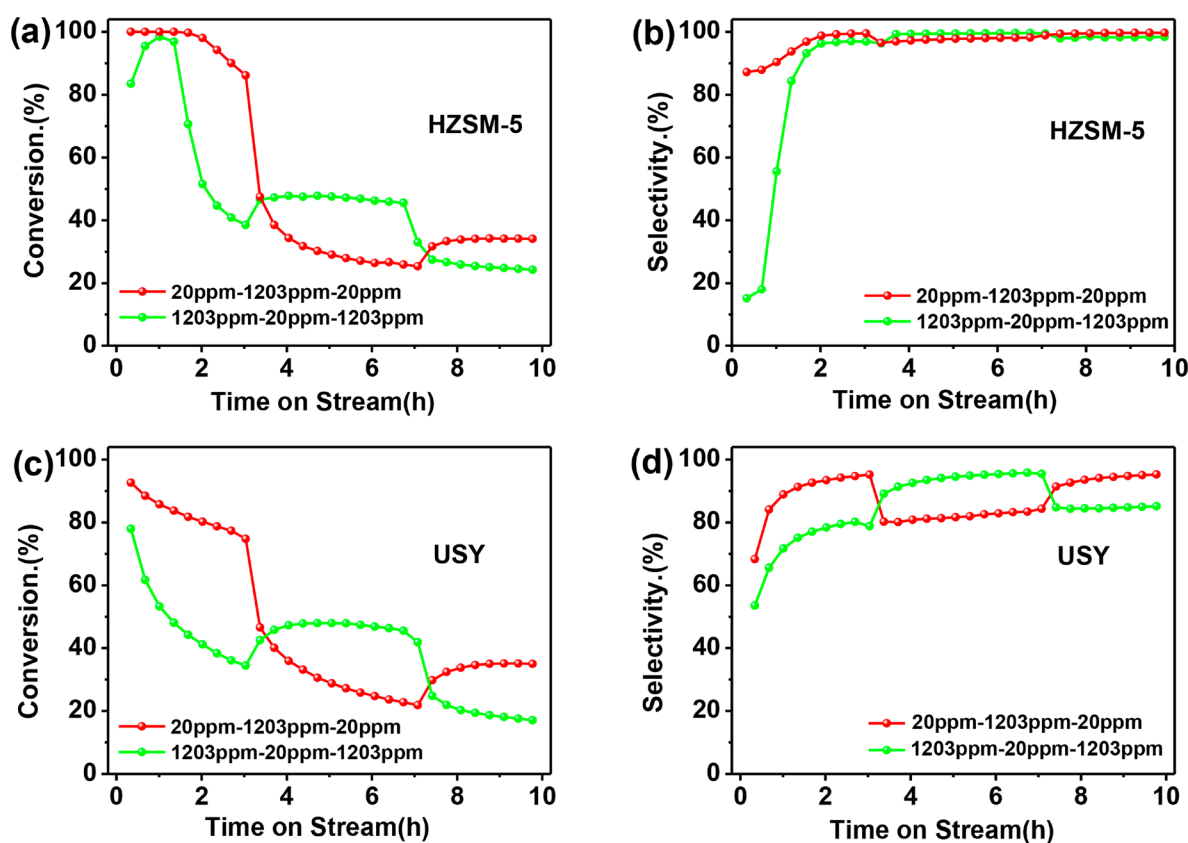
Figure 3. (a, c) EDC conversion and (b, d) the selectivity of VCM over zeolite catalysts by in situ feedstock switching. Reaction conditions: WHSV = 0.5 h⁻¹, zeolite: (a, b) HZSM-5, (c, d) USY, 300 °C, 0.1 MPa, N₂/CH₂ClCH₂Cl = 19/1, feedstock switching at the third and seventh hour.

2) showing that the involvement of water molecules leads to changes in the acidity of zeolites.

The IR spectra show that the involvement of water molecules in the EDC feedstock led to a change in the Bronsted acid site to Lewis acid site ratio during the reaction, which may be the main reason for the rapid deactivation of the zeolite catalyst in the presence of water. To verify this conclusion, we carried out feedstock switching experiments, as shown in Figure 3.

Figure 3 shows the feedstock switching experiments performed on the USY and HZSM-5 catalyst. Using EDC (20 ppm water) and EDC (1203 ppm water) as initial feedstocks, the reaction was carried out for 3 h by rapidly switching the initial feedstock to the other feedstock and then switching back to the initial feedstock after 4 h of reaction. When EDC with 20 ppm water was used as the feedstock, the EDC conversion and VCM selectivity decreased rapidly as the feedstock was switched the first time. After the feedstock was switched the second time, the EDC conversion was improved, but the value was much lower than that before feedstock switching, while the VCM selectivity increased to the same value observed before feedstock switching (Figure 1). In contrast, when EDC with 1203 ppm water was used as the initial feedstock, the EDC conversion only slightly increased by 10−20% after switching the feedstock the first time, and the VCM selectivity increased to the same value as that observed with the feedstock containing 20 ppm water. After the feedstock was switched the second time, both the EDC conversion and VCM selectivity decreased again to the corresponding results of the feedstock with 1203 ppm water.

The two types of switching tests again reveal that the activity of zeolites was strongly influenced by the water content in the EDC feedstock. This is consistent with Shalygin,[9] who reported that Bronsted acids easily form oligomers, which led to rapid zeolite deactivation, and with the previous findings of IR characterizations suggesting that a dynamic transition from Lewis acid sites to Bronsted acid sites took place on the zeolite catalyst in the presence of water molecules.

In addition to the above experiments, theoretical calculations were also carried out to study the effect of water on the adsorption of reactants and products on zeolites. The host−guest interactions between zeolites (MFI, FAU) and EDC or VCM were also investigated by density functional theory (DFT) calculations.[32−34] Two conditions, aqueous and anhydrous, were selected for detailed analysis. The calculations show that the interaction energies were all enhanced with the involvement of water molecules. By introducing water molecules into the zeolite-EDC system, the interaction energy (Table S2) of substances decreased. The interaction energy between the zeolite and water was much lower than the interaction energy between the zeolite and EDC. This indicates that H_2O preferentially adsorbed on the zeolites and coadsorbed with EDC. In addition, the interaction energy calculations were extended to the zeolite-VCM system. The interaction energy (Figure 4) of MFI with water molecules and VCM molecules was -0.11×10^3 kcal/mol, while the interaction energy of MFI with VCM was -0.09×10^3 kcal/mol. Meanwhile, the interaction energy of FAU with water and VCM was -0.03×10^3 kcal/mol, while the interaction energy of FAU with VCM was -0.01×10^3 kcal/mol. The above theoretical calculation results indicate that the presence of
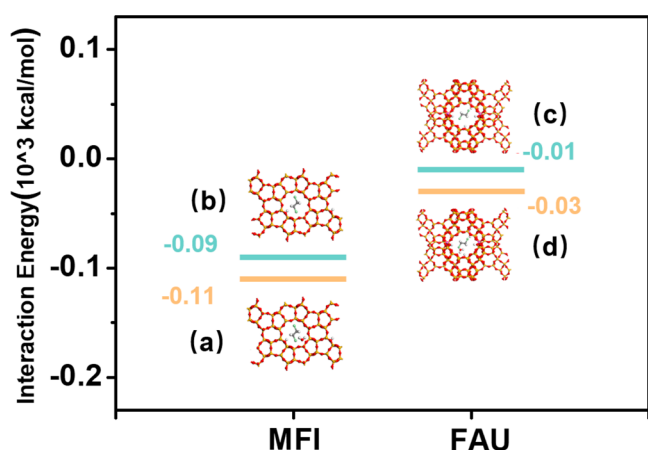
Figure 4. Optimized conformational geometries and interaction energy. Conformational geometries: (a) MFI/VCM-H$_2$O, (b) MFI/VCM, (c) FAU/VCM, and (d) FAU/VCM-H$_2$O (white, H; red, O; yellow, Si; lavender, Al; green, Cl; and gray, C).

water enhances the adsorption of EDC and VCM on the zeolites, which has an important impact on the catalytic performance of zeolites. In particular, the adsorption of the VCM product reduces the selectivity for EDC cracking, accelerates carbon deposition on the zeolites, and thus accelerates the deactivation of the catalysts.

CONCLUSION

In conclusion, it was found for the first time that the presence of trace water in EDC feedstock had a significant negative impact on the catalytic performance of zeolite catalysts in the catalytic cracking of EDC to produce VCM. FTIR, Py-FTIR, thermogravimetry, solid-state NMR, feedstock switching tests, and TDDFT calculations revealed that the presence of trace water in the EDC feedstock easily affects the Bronsted acid site to Lewis acid site ratio of zeolites and tends to enhance the adsorption of EDC or VCM on zeolites, which together lead to a decrease in the catalyst activity, selectivity, and stability of zeolite catalysts for the catalytic cracking of EDC to produce VCM. This study provides a new idea for follow-up research by showing that strictly controlling the water content in EDC can help improve the activity, selectivity, and most importantly, the stability of the EDC catalytic cracking reaction.

ASSOCIATED CONTENT

SI **Supporting Information**

The Supporting Information is available free of charge at https://pubs.acs.org/doi/10.1021/acs.iecr.2c02918.

> Additional data regarding the catalyst characterization, catalyst evaluation, and switching experiment (PDF)

AUTHOR INFORMATION

Corresponding Author

Yunpeng Xu − *National Engineering Research Center of Lower-Carbon Catalysis Technology, Dalian National Laboratory for Clean Energy, Dalian Institute of Chemical Physics, Chinese Academy of Sciences, Dalian 116023 Liaoning, China;* ◎ orcid.org/0000-0002-5165-5803; Email: xuyunpeng@dicp.ac.cn

Authors

Quan Zhang − *University of Chinese Academy of Sciences, Beijing 100049, China; National Engineering Research Center of Lower-Carbon Catalysis Technology, Dalian National Laboratory for Clean Energy, Dalian Institute of Chemical Physics, Chinese Academy of Sciences, Dalian 116023 Liaoning, China*

Wei Huang − *National Engineering Research Center of Lower-Carbon Catalysis Technology, Dalian National Laboratory for Clean Energy, Dalian Institute of Chemical Physics, Chinese Academy of Sciences, Dalian 116023 Liaoning, China*

Jiacheng Xing − *National Engineering Research Center of Lower-Carbon Catalysis Technology, Dalian National Laboratory for Clean Energy, Dalian Institute of Chemical Physics, Chinese Academy of Sciences, Dalian 116023 Liaoning, China*

Xingzong Dong − *University of Chinese Academy of Sciences, Beijing 100049, China; National Engineering Research Center of Lower-Carbon Catalysis Technology, Dalian National Laboratory for Clean Energy, Dalian Institute of Chemical Physics, Chinese Academy of Sciences, Dalian 116023 Liaoning, China*

Guangye Liu − *National Engineering Research Center of Lower-Carbon Catalysis Technology, Dalian National Laboratory for Clean Energy, Dalian Institute of Chemical Physics, Chinese Academy of Sciences, Dalian 116023 Liaoning, China*

Zhongmin Liu − *University of Chinese Academy of Sciences, Beijing 100049, China; National Engineering Research Center of Lower-Carbon Catalysis Technology, Dalian National Laboratory for Clean Energy, Dalian Institute of Chemical Physics, Chinese Academy of Sciences, Dalian 116023 Liaoning, China;* ◎ orcid.org/0000-0002-7999-2940

Complete contact information is available at:
https://pubs.acs.org/10.1021/acs.iecr.2c02918

Notes
The authors declare no competing financial interest.

ACKNOWLEDGMENTS

REFERENCES

(1) Song, Z.; Liu, G.; He, D.; Pang, X.; Tong, Y.; Wu, Y.; Yuan, D.; Liu, Z.; Xu, Y. Acetylene Hydrochlorination over 13x Zeolite Catalysts at High Temperature. *Green Chem.* **2016**, *18*, 5994−5998.

(2) Lin, R.; Amrute, A. P.; Perez-Ramirez, J. Halogen-Mediated Conversion of Hydrocarbons to Commodities. *Chem. Rev.* **2017**, *117*, 4182−4247.

(3) Huybrechts, G.; Wouters, G. Mechanism of the Pyrolysis of 1,2-Dichloroethane in the Absence and Presence of Added Chlorine. *International Journal of Chemical Kinetics* **2002**, *34*, 316−321.

(4) Chen, C.; Shen, Z. B.; Zhu, Y. P.; Wang, F.; Jiang, B.; Qi, H. M. Construction of Activated Carbon-Supported B3n3 Doped Carbon as Metal-Free Catalyst for Dehydrochlorination of 1,2-Dichloroethane to Produce Vinyl Chloride. *Rsc Advances* **2021**, *11*, 183−191.

(5) Wang, J.; Fan, S. S.; Duan, H. M.; Xu, J. M.; Huang, Y. Q. Anion Exchange Resin Based Porous Carbon Spheres for the Catalytic 1,2-Dehydrochlorination of Dichloroethane. *J. Phys. Chem. C* **2021**, *125*, 24422−24428.

(6) Shen, Z. B.; Han, Y. J.; Liu, Y.; Qin, Y. J.; Xing, P.; Zhao, H.; Jiang, B. Understanding Surface Basic Sites of Catalysts: Kinetics and Mechanism of Dehydrochlorination of 1,2-Dichloroethane over N-Doped Carbon Catalysts. *Catalysts* **2020**, *10*, 707.

(7) Magistro, A. J., Catalytic Dehydrohalogenation Catalyst. U.S. Patent 07372589, 1989.

(8) Testova, N. V.; Shalygin, A. S.; Glazneva, T. S.; Paukshtis, E. A.; Parmon, V. N. Unusual 1,2-Dichloroethane Dehydrochlorination over Ruthenium-Oxychloride Catalyst. *Catal. Commun.* **2015**, *67*, 95−97.

(9) Shalygin, A. S.; Malysheva, L. V.; Paukshtis, E. A. Mechanism of 1,2-Dichloroethane Dehydrochlorination on the Acid Sites of Oxide Catalysts as Studied by Ir Spectroscopy. *Kinetics and Catalysis* **2011**, *52*, 305−315.

(10) Bai, S. X.; Dai, Q. G.; Chu, X. X.; Wang, X. Y. Dehydrochlorination of 1,2-Dichloroethane over Ba-Modified Al2o3 Catalysts. *Rsc Advances* **2016**, *6*, 52564−52574.

(11) Baran, R.; Srebowata, A.; Kaminska, I. I.; Lomot, D.; Dzwigaj, S. Catalytic Activity of Halbea and Ni(X)Halbea Zeolites in Hydrogen-Assisted Dehydrochlorination of 1,2-Dichloroethane into Vinyl Chloride Monomer. *Microporous Mesoporous Mater.* **2013**, *180*, 209−218.

(12) Srebowata, A.; Baran, R.; Kaminska, I. I.; Onfroy, T.; Krafft, J. M.; Dzwigaj, S. Catalytic Hydrogen-Assisted Dehydrochlorination of 1,2-Dichloroethane over Cobalt-Containing Beta Zeolite. *Catal. Today* **2015**, *251*, 73−80.

(13) Sotowa, C.; Watanabe, Y.; Yatsunami, S.; Korai, Y.; Mochida, I. Catalytic Dehydrochlorination of 1,2-Dichloroethane into Vinyl Chloride over Polyacrylonitrile-Based Active Carbon Fiber. *Appl. Catal. A-Gen.* **1999**, *180*, 317−323.

(14) Zhao, W.; Sun, M. X.; Zhang, H. Y.; Dong, Y. Z.; Li, X. Y.; Li, W.; Zhang, J. L. Catalytic Dehydrochlorination of 1,2-Dichloroethane to Produce Vinyl Chloride over N-Doped Coconut Activated Carbon. *RSC Adv.* **2015**, *5*, 104071−104078.

(15) Zhao, W.; Li, W.; Zhang, J. Ru/N-Ac Catalyst to Produce Vinyl Chloride from Acetylene and 1,2-Dichloroethane. *Catalysis science & technology* **2016**, *6*, 1402−1409.

(16) Boudewijns, T.; Piccinini, M.; Degraeve, P.; Liebens, A.; De Vos, D. Pathway to Vinyl Chloride Production Via Dehydrochlorination of 1,2-Dichloroethane in Ionic Liquid Media. *ACS Catal.* **2015**, *5*, 4043−4047.

(17) Cook, S. E.; Neher, C. M., Process of Making Ethyl Chloride and Vinyl Chloride. U.S. Patent 2838577A, 1957.

(18) Cejka, J.; Jiru, P. Influence of Water on Activity, Selectivity and Deactivation of Zeolites in Acetone Transformation. *Collect. Czech. Chem. Commun.* **1989**, *54*, 2998−3002.

(19) Wang, X. Y.; Wen, M.; Wang, C. Z.; Ding, J.; Sun, Y.; Liu, Y.; Lu, Y. Microstructured Fiber@Hzsm-5 Core-Shell Catalysts with Dramatic Selectivity and Stability Improvement for the Methanol-to-Propylene Process. *Chem. Commun.* **2014**, *50*, 6343−6345.

(20) Zhao, S. F.; Yang, D.; Zhang, X. W.; Yao, X. T.; Liu, Y. M.; He, M. Y. Zsm-5 with Controllable Acidity as an Efficient Catalyst for a Highly Adjustable Propene/Ethene Ratio in the 1-Butene Cracking. *Chem. Commun.* **2016**, *52*, 11191−11194.

(21) Arora, S. S.; Nieskens, D. L. S.; Malek, A.; Bhan, A. Lifetime Improvement in Methanol-to-Olefins Catalysis over Chabazite Materials by High-Pressure H-2 Co-Feeds. *Nature Catalysis* **2018**, *1*, 666−672.

(22) Zhao, X. B.; Li, J. Z.; Tian, P.; Wang, L. Y.; Li, X. F.; Lin, S. F.; Guo, X. W.; Liu, Z. M. Achieving a Superlong Lifetime in the Zeolite-Catalyzed Mto Reaction under High Pressure: Synergistic Effect of Hydrogen and Water. *ACS Catal.* **2019**, *9*, 3017−3025.

(23) Li, Z. B.; Martinez-Triguero, J.; Yu, J. H.; Corma, A. Conversion of Methanol to Olefins: Stabilization of Nanosized Sapo-34 by Hydrothermal Treatment. *J. Catal.* **2015**, *329*, 379−388.

(24) Ibarra, A.; Veloso, A.; Bilbao, J.; Arandes, J. M.; Castano, P. Dual Coke Deactivation Pathways During the Catalytic Cracking of Raw Bio-Oil and Vacuum Gasoil in Fcc Conditions. *Appl. Catal., B* **2016**, *182*, 336−346.

(25) Bollini, P.; Chen, T. T.; Neurock, M.; Bhan, A. Mechanistic Role of Water in Hssz-13 Catalyzed Methanol-to-Olefins Conversion. *Catalysis Science & Technology* **2019**, *9*, 4374−4383.

(26) Sun, J. M.; Baylon, R. A. L.; Liu, C. J.; Mei, D. H.; Martin, K. J.; Venkitasubramanian, P.; Wang, Y. Key Roles of Lewis Acid-Base Pairs on Znxzryoz in Direct Ethanol/Acetone to Isobutene Conversion. *J. Am. Chem. Soc.* **2016**, *138*, 507−517.

(27) Zecchina, A.; Bordiga, S.; Spoto, G.; Marchese, L.; Petrini, G.; Leofanti, G.; Padovan, M. Silicalite Characterization. 1. Structure, Adsorptive Capacity, and Ir Spectroscopy of the Framework and Hydroxyl Modes. *J. Phys. Chem.* **1992**, *96*, 4985−4990.

(28) Bordiga, S.; Ugliengo, P.; Damin, A.; Lamberti, C.; Spoto, G.; Zecchina, A.; Spano, G.; Buzzoni, R.; Dalloro, L.; Rivetti, F. Hydroxyls Nests in Defective Silicalites and Strained Structures Derived Upon Dehydroxylation: Vibrational Properties and Theoretical Modelling. *Top. Catal.* **2001**, *15*, 43−52.

(29) Jiang, M.; Karge, H. G. Investigation of Acid Properties of Dealuminated H-Mordenite Zeolites by Low-Temperature Diffuse Reflectance Ftir. *Journal of the Chemical Society-Faraday Transactions* **1996**, *92*, 2641−2649.

(30) Deruiter, R.; Kentgens, A. P. M.; Grootendorst, J.; Jansen, J. C.; Vanbekkum, H. Calcination and Deboronation of B -Mfi Single-Crystals. *Zeolites* **1993**, *13*, 128−138.

(31) Emeis, C. A. Determination of Integrated Molar Extinction Coefficients for Infrared-Absorption Bands of Pyridine Adsorbed on Solid Acid Catalysts. *J. Catal.* **1993**, *141*, 347−354.

(32) Delley, B. An All-Electron Numerical-Method for Solving the Local Density Functional for Polyatomic-Molecules. *J. Chem. Phys.* **1990**, *92*, 508−517.

(33) Delley, B. From Molecules to Solids with the Dmol(3) Approach. *J. Chem. Phys.* **2000**, *113*, 7756−7764.

(34) Jacquemin, D.; Wathelet, V.; Perpete, E. A.; Adamo, C. Extensive Td-Dft Benchmark: Singlet-Excited States of Organic Molecules. *J. Chem. Theory Comput.* **2009**, *5*, 2420−2435.

▣ Recommended by ACS